Theoretical Constraints for Observation of Superdeformed Bands in the Mass-60 Region

Yang Sun,[1] Jing-ye Zhang,[1] Mike Guidry,[1] and Cheng-Li Wu[2]
[1]*Department of Physics and Astronomy, University of Tennessee, Knoxville, Tennessee 37996*
[2]*Department of Physics, Chung Yuan Christian University, Chung-Li, Taiwan 32023, Republic of China*
(Received 26 January 1999)

The lightest superdeformed nuclei of the mass-60 region are described using the projected shell model. In contrast to the heaviest superdeformed nuclei where a coherent motion of nucleons often dominates the physics, it is found that alignment of $g_{9/2}$ proton and neutron pairs determines the high spin behavior for superdeformed rotational bands in this mass region. It is predicted that, due to the systematics of shell fillings along the even-even Zn isotopic chain, observation of a regular superdeformed yrast band sequence will be unlikely for certain nuclei in this mass region.

PACS numbers: 21.10.Re, 21.60.Cs, 23.20.Lv, 27.50.+e

The mass-190 nuclei are the heaviest nuclei known where long-sequence rotational bands associated with the superdeformed (SD) minimum have been observed [1]. In a recent systematic study using the projected shell model (PSM) [2], it was concluded that the role of high-j intruder orbitals is suppressed in these nuclei because of strong correlations in the quadrupole field and non-negligible correlations in the pair field [3]. This conclusion was reinforced by the demonstration that quasiparticle additivity generally does not hold [4]. Superdeformation in the mass-60 region was predicted some years ago [5] and was recently observed [6–8]. This is the lightest known region of SD rotational bands and these new bands show very different character from those of the mass-190 nuclei.

The mass-60 SD bands are associated with the highest rotational frequencies ($\hbar\omega \approx 1.8$ MeV) observed so far in SD nuclear systems; in contrast, in the SD mass-190 nuclei the maximum rotational frequency is typically 0.4 MeV. However, the magnitudes of deformation and pairing appear to be comparable in the mass-60 and mass-190 regions. We may expect that the single-particle level density near the $N = 30$ gap is much lower than for heavier nuclei. Thus, there can be substantial fluctuations in shell fillings along an isotopic chain, which could give rise to drastic changes in the single particle and collective behavior. In addition, the maximum spin within the yrast and near-yrast bands in SD mass-60 nuclei is generally much lower than in heavier nuclei (SD bands terminate earlier [9]). These new features lead us to expect complex behavior in this region relative to previously studied SD nuclei.

Thus far, the SD bands of the mass-60 nuclei have been explained using mean-field theories (cranked relativistic mean-field theory and cranked Nilsson model [9], or cranked Skyrme-Hartree-Fock method [7]), with complete neglect of pairing correlations. These descriptions reproduce many of the gross features found in these nuclei. However, some interesting questions have not been discussed. For example, why does the observed SD band in ^{62}Zn [6] consist of only a few γ rays, while population of the SD band in neighboring ^{60}Zn [8] extends to low spin states? And why has one not seen a SD yrast band at all in ^{64}Zn [10]? Can one predict spin values for these bands? Can one give a microscopic justification for the complete neglect of pairing in all calculations reported prior to this one?

In an investigation using the PSM, we have found a surprisingly good description of the SD behavior in this region and rather plausible answers to these questions in terms of band crossings and band interactions involving the $g_{9/2}$ intruder orbits. Because of high angular momentum j, the fully paired $g_{9/2}$ quasiparticles in the ground state are most strongly affected by the Coriolis antipairing force when the nucleus rotates. The pairs break during the rotation and align their spins along the direction of the collective rotation. Viewed in terms of bands, a 2-quasiparticle (2-qp) band (or a band with a broken pair) which lies higher in energy at zero rotation becomes lower at a certain angular momentum than the ground band. Thus, band crossing is related to the microscopic alignment process, and can be linked to experimental observations. In this Letter, we concentrate our discussion on the important physical consequences of our interpretation, leaving general results of our investigation to be published elsewhere.

The PSM has been successfully applied to normally deformed nuclei [2] as well as SD nuclei in various mass regions [3,11]. For details of the PSM theory we refer to the review article of Hara and Sun [2] and to the published computer code [12]. In the PSM, the many-body wave function is a superposition of (angular momentum) projected multi-quasi-particle states,

$$|\psi_M^I\rangle = \sum_\kappa f_\kappa \hat{P}^I_{MK_\kappa} |\varphi_\kappa\rangle, \qquad (1)$$

where $|\varphi_\kappa\rangle$ denotes basis states consisting of the quasiparticle (qp) vacuum, two quasineutron and quasiproton, and four qp states for even-even nuclei. The dimension of the qp basis in the present calculation is about 50. Since ^{60}Zn has a deformation of $\beta_2 = 0.47$ [8], the deformation of our basis is fixed at $\epsilon_2 = 0.45$ for all nuclei calculated in this paper. Three full major shells ($N = 2$, 3, and 4)

 0031-9007/99/83(4)/686(4)$15.00

are employed for neutrons and for protons (with a frozen ^{16}O core). For the Nilsson parameters κ and μ we take the values of Ref. [13]. Two-body interactions are then diagonalized in the basis generated using the above deformed mean field with angular momentum projection.

We use the usual separable-force Hamiltonian [2],

$$\hat{H} = \hat{H}_0 - \frac{\chi}{2} \sum_{\mu} \hat{Q}^{+}_{\mu} \hat{Q}_{\mu} - G_M \hat{P}^{+} \hat{P} - G_Q \hat{P}^{+}_{\mu} \hat{P}_{\mu} , \quad (2)$$

with spherical single-particle, residual quadrupole-quadrupole, monopole pairing, and quadrupole pairing terms. The strength χ of the quadrupole-quadrupole term is fixed self-consistently with the deformation, so it is not a true parameter [14]. Lack of SD data precludes determining the pairing interaction strength from experimental odd-even mass differences in a systematic way, so we have used the prescription introduced in Ref. [11], which corresponds in this case to multiplying the monopole pairing strengths G_M of Ref. [13] by 0.90 to accommodate the relative increase in the size of the basis for the present calculation. This amount of reduction is consistent with the principles described in Ref. [15]. For the quadrupole pairing interaction G_Q, a ratio $C = G_Q/G_M = 0.28$ is used, the same value used in the heavy SD nuclei [3].

To illustrate the physics, the calculated band diagram (energy for the projected basis states in Eq. (1) as a function of spin; see Ref. [2] for a further interpretation of this diagram) is shown in Fig. 1 for ^{60}Zn. The 2-qp states correspond to the group of bands starting at about 4–5 MeV in energy (solid lines for neutrons and dotted lines for protons). Among these bands, we observe that two behave in a unique way: at the bandhead they lie a little higher than the other 2-qp bands, but rapidly decrease relative to the other bands as the system rotates. Thus, in the initial band crossing region these two bands are on average 2 MeV lower than the other 2-qp bands. The 2-qp states exhibiting this behavior correspond to the neutron and the proton 2-qp state coupled from $K = \frac{1}{2}$ and $K = \frac{3}{2}$ particles in the $g_{9/2}$ orbital to a total $K = 1$. The band corresponding to the $g_{9/2}$ proton 2-qp states crosses the ground band (the first band crossing) and becomes the lowest band beyond $I = 14$.

A group of 4-quasiparticle (4-qp) states is illustrated in Fig. 1 as the set of dashed lines starting at about 8–9 MeV. One of these that is flat in the low spin region is constructed from the above-mentioned two $g_{9/2}$ pairs of neutrons and protons that are the most favorable 2-qp states in energy. The $g_{9/2}$ proton 2-qp band is crossed between $I = 18$ and 20 by this 4-qp state (the second band crossing). Thus, the important multi-quasi-particle states that lie lowest in energy for the spin range to be considered are composed entirely from $g_{9/2}$ orbitals, and we may expect that quasiparticle states from other orbitals (e.g., $f_{7/2}$ or $p_{3/2}$) will play a less important role near the yrast line.

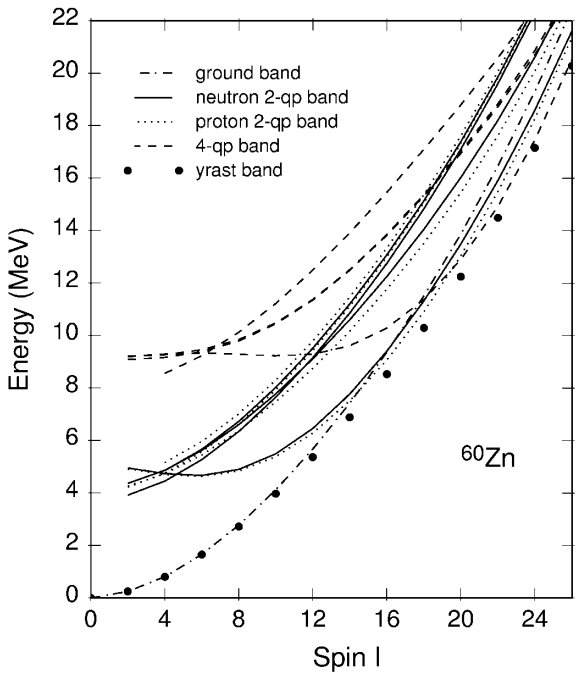

FIG. 1. Band diagram calculated for SD ^{60}Zn. Black dots are the yrast states after band mixing at each spin, which are used to plot the theoretical curves in Figs. 2 and 3.

From the preceding discussion, we conclude that high spin physics near the yrast line in the SD even-even, mass-60 nuclei should be governed by crossings and interactions between bands built upon neutron and proton $g_{9/2}$ quasiparticles. Because the single-particle state density is low, we may further expect the influence of band crossings and interactions to fluctuate drastically along isotopic chains. On the other hand, states built upon quasiparticles from other orbitals occur at much higher energies. They can contribute to the collective quantities (e.g., the collective portion of the angular momentum and the total electric quadrupole moment), but not strongly to quantities dominated by the quasiparticle properties.

We show the calculated energy spectra in terms of the transitional energy E_γ in Fig. 2 and dynamical moments of inertia $\Im^{(2)}$ in Fig. 3 for the even-even isotopic chain $^{60-66}$Zn. Comparisons with experimental data are shown where data are available. For ^{60}Zn, both E_γ and $\Im^{(2)}$ agree reasonably well with data (data has the peak at $I = 20$, while the calculated one is at $I = 18$). The SD band in ^{60}Zn is linked experimentally to the known low-lying states [8], so the spin of this band is known. Thus this agreement supports the choices of interaction strengths used in the present calculation. We can then predict spins for other SD bands where no linking transitions are observed. For ^{62}Zn, the best agreement between theory and data corresponds to placing the measured first SD E_γ at $I = 20$ (see Fig. 2), thus predicting this transition to be from the state $I = 20$ to $I = 18$. This agrees with the assignment proposed previously by Afanasjev *et al.* [9].

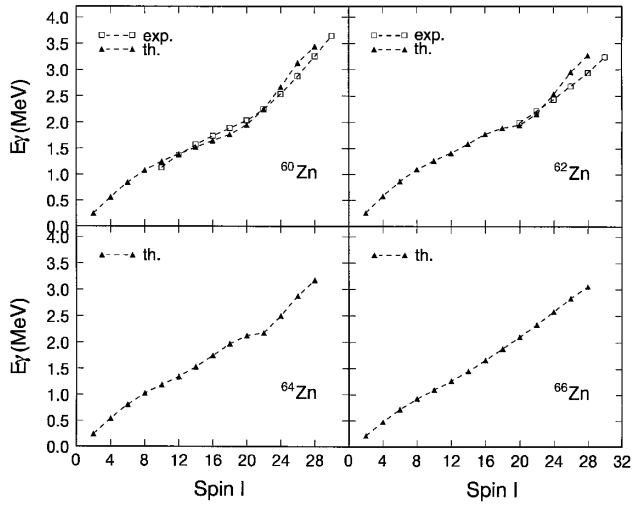

FIG. 2. The PSM results for $E_\gamma(I) = E(I) - E(I-2)$ in SD yrast bands, and comparison with experiment where data are available (Ref. [8] for ^{60}Zn and Ref. [6] for ^{62}Zn).

In Fig. 3, there are in general two peaks in the $\Im^{(2)}$ plots that reflect the two successive band crossings discussed above. The first occurs at $I \approx 12$, with the location and size being similar for each of the four isotopes. This is because the first crossing is mainly the $g_{9/2}$ proton pair crossing, which is relatively constant within this isotopic chain. However, the next band crossing, caused by a 4-qp state of $g_{9/2}$ neutron and proton pairs, leads to very different consequences for each individual SD band; this implies significant theoretical constraints for the possibility of observation, as we now discuss.

The projected shell model is known to give a good description of band crossings in heavier nuclei where it has been tested extensively (for example, see Ref. [16]).

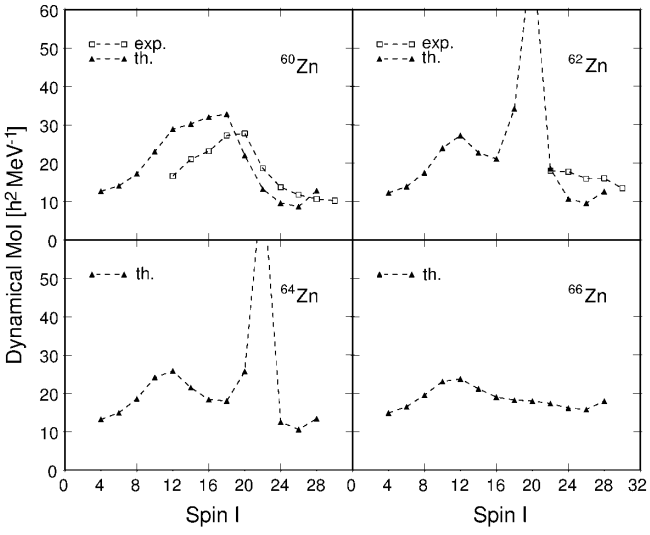

FIG. 3. The PSM results for $\Im^{(2)}(I) = 4/[E_\gamma(I) - E_\gamma(I-2)]$ in SD yrast bands, and comparison with experiment where data are available.

The nature of the crossing (e.g., whether the peak in $\Im^{(2)}$ is sharp or gentle) is related to the angle between crossing bands [2]. A small angle spreads the interaction over a wide angular momentum range, thus producing a smoother change. A large angle implies that the bands interact over a narrow angular momentum range, and a sudden discontinuity can occur. In our case, a smaller crossing angle is seen just before $I = 20$ for ^{60}Zn, producing a smoothed interaction (see Fig. 1). In fact, the two peaks in $\Im(2)$ caused by first and second band crossings merge in this case, resulting in one wide and smooth peak ranging from low to high spins. However, a larger crossing angle is found at $I = 20$ for ^{62}Zn. Thus, in the $\Im(2)$ plot for ^{62}Zn a clear separation of the two peaks is seen, with the second one at $I = 20$ being much higher. If this discontinuity is pronounced, it may be expected to set a lower limit in angular momentum for observation of such a SD band with weak intensity, while the upper limit is determined by the band termination spin [9]. This explains succinctly why the observed SD band in ^{60}Zn is long, while in the neighboring ^{62}Zn, where one might naively expect similar behavior, the observed band is very short.

Galindo-Uribarri *et al.* reported a rotational SD band in ^{64}Zn [10]. Because of the strong dipole transitions discovered in their work, this band appears not to belong to the same type of bands (SD yrast bands characterized by even integer spins only) discussed above [17]. An important question is why the usual SD yrast band has not been seen in ^{64}Zn. We find that, due to different neutron shell fillings, the position of the $g_{9/2}$ neutron 2-qp band is shifted higher in energy for this case, which in turn pushes the 4-qp band higher. Consequently, the second band crossing spin is shifted to $I = 22$, a spin which is even closer to the band termination. In addition, this second band crossing is very sharp (see Fig. 3). If the experimental analysis were not able to follow the population over the sharp second band crossing, there would be at most three or four transitional gamma rays to measure, making observation of the SD yrast band in this nucleus difficult.

Going to the next isotope, ^{66}Zn, a different picture appears. Because of the shift in neutron Fermi level, the pair of $g_{9/2}$ neutrons contributing to the 4-qp state is changed from $K = \frac{1}{2}$ and $K = \frac{3}{2}$ particles to $K = \frac{3}{2}$ and $K = \frac{5}{2}$ (still coupled to total $K = 1$). Because of the even higher energy and steeper curvature of this 4-qp band, we find that it crosses the proton 2-qp band at $I = 26$ at a very small angle. In fact, one can hardly see in the $\Im^{(2)}$ plot that there is a band crossing. Thus, our calculation suggests that there should be a much better chance to observe a long SD yrast band in ^{66}Zn, where no experiment has yet been reported [17].

It has been demonstrated previously [16] that the position of band crossings can be shifted systematically to higher spin by a stronger quadrupole pairing interaction. Therefore, the discrepancy mentioned in the $\Im(2)$ plot in

the ^{60}Zn calculation (the theoretical peak occurs two spin units too early) could be improved if a larger quadrupole pairing interaction were employed. We have not introduced this refinement because for this particular $N = Z$ nucleus we may expect that neutron-proton pairing correlations may also play a role. For example, Ref. [18] found that the $T = 0$ pairing becomes significant at very high spins (where the $g_{9/2}$ orbital became important) in the lighter $N = Z$ nucleus ^{48}Cr. This neutron-proton pairing has not been included in the present calculation or in the calculations of Refs. [7,9]. Explicitly including the *p-n* pairing in the PSM is of interest for future work.

When we calculate the pairing gaps using the total many-body wave function, we find that both neutron and proton pairing is significant at $I = 0$ (gaps of about 0.9 MeV). However, there is a rapid drop in pairing gaps near the first band crossing. Beyond $I = 18$, they assume small, nearly constant values corresponding to about 40% of their initial values. All measured SD bands in the mass-60 region are in the spin range beyond $I = 18$. Thus, our results may provide an understanding of the success of mean-field calculations, all of which have neglected pairing correlations completely [7,9]. Details will be reported in a forthcoming paper.

In summary, the projected shell model has been used to carry out the first study of SD mass-60 even-even nuclei using techniques that go beyond the mean field. In contrast to the heaviest SD systems, where coherent motion of many nucleons is important and alignment in specific orbits is less significant, it is found that alignment of $g_{9/2}$ proton and neutron pairs dominates the high spin behavior in these lightest SD nuclei. Because of this, and the low level densities expected for this mass region near the Fermi surface, we find that the nature of the SD bands can fluctuate strongly with shell filling in even-even isotopic sequences. Calculations for the even-even Zn isotopic chain provide an explanation for the bands already observed, and make specific predictions about which nuclei are the best candidates for long rotational SD sequences in this region. Because our calculations go beyond the mean field, they can be used to check various assumptions of the mean-field descriptions. For example, we have calculated the pairing gaps dynamically and find that they generally are not small at low spins, but drop rapidly to nonzero but relatively small values in the region where data are available, thus providing a partial microscopic justification for the uniform neglect of pairing in all mean-field calculations reported to date. Finally, for the only case in this region where the spin has been measured, our calculated spin agrees with the measured spin without parameter adjustment. This, coupled with numerous previous correct predictions of spin for SD bands in the mass-130 and mass-190 nuclei, permits us to predict theoretical spins with confidence for those cases where they have not yet been measured.

Valuable discussions with A. Galindo-Uribarri, P. Ring, A. V. Afanasjev, and D. J. Hartley are acknowledged. One of us (J.-y. Z.) is supported by the U.S. Department of Energy through Contract No. DE-FG05-96ER40983.

[1] X.-L. Han and C.-L. Wu, At. Data Nucl. Data Tables **63**, 117 (1996); B. Singh, R. B. Firestone, and S. Y. F. Chu, Nucl. Data Sheets **78**, 1 (1996).
[2] K. Hara and Y. Sun, Int. J. Mod. Phys. E **4**, 637 (1995).
[3] Y. Sun, J.-y Zhang, and M. Guidry, Phys. Rev. Lett. **78**, 2321 (1997).
[4] J.-y. Zhang, Y. Sun, L. L. Riedinger, and M. Guidry, Phys. Rev. C **58**, 868 (1998).
[5] I. Ragnarsson, Proceedings of the Workshop on the Science of Intense Radioactive Ion Beams, edited by J. B. McClelland and D. J. Vieira (unpublished) (Los Alamos National Laboratory Report LA-11964-C, 1990), p. 199.
[6] C. E. Svensson *et al.*, Phys. Rev. Lett. **79**, 1233 (1997); **80**, 2558 (1998).
[7] D. Rudolph *et al.*, Phys. Rev. Lett. **80**, 3018 (1998).
[8] C. E. Svensson *et al.*, Phys. Rev. Lett. **82**, 3400 (1999).
[9] A. V. Afanasjev, I. Ragnarsson, and P. Ring, Phys. Rev. C **59**, 3166 (1999).
[10] A. Galindo-Uribarri *et al.*, Phys. Lett. B **422**, 45 (1998).
[11] Y. Sun and M. Guidry, Phys. Rev. C **52**, R2844 (1995).
[12] Y. Sun and K. Hara, Comput. Phys. Commun. **104**, 245 (1997).
[13] T. Bengtsson and I. Ragnarsson, Nucl. Phys. **A436**, 14 (1985).
[14] V. Velázquez, J. Hirsch, and Y. Sun, Nucl. Phys. **A643**, 39 (1998).
[15] Z. Szymański, Nucl. Phys. **28**, 63 (1961).
[16] Y. Sun, S. X. Wen, and D. H. Feng, Phys. Rev. Lett. **72**, 3483 (1994).
[17] A. Galindo-Uribarri (private communication).
[18] J. Terasaki, R. Wyss, and P.-H. Heenen, Phys. Lett. B **437**, 1 (1998).